


Switching between slow light and fast light by static magnetic field in a degenerate four-level atomic system at room temperature

Nguyen Van Phu, Nguyen Huy Bang , Luong Thi Yen Nga and Le Van Doai* 

Vinh University, 182 Le Duan Street, Vinh City, Vietnam

E-mail: doailv@vinhuni.edu.vn

Received 8 November 2023, revised 17 April 2024

Accepted for publication 3 May 2024

Published 15 May 2024



Abstract

The optical response of a magnetic-degenerated four-level atom system to the two left and right circular polarization components of the probe field is represented at room temperature. The absorption spectrum and group index for the two polarization components of the probe field are controlled according to the static magnetic field and the coupling field under electromagnetically induced transparency condition. By varying the strength of the static magnetic field, the optical response of the atomic medium can be changed from transparency to absorption or vice versa and hence the amplitude of group index also changes from positive extreme to negative extreme or vice versa. The same phenomenon also occurs when changing the coupling field intensity. In addition, temperature also significantly influence on the optical response of the atomic medium, which changes not only the amplitude but also the sign of the group index as the temperature increases. Our analytical results can be useful for experimental observation and related applications of light group index/velocity at room temperature.

Keywords: electromagnetically induced transparency, group index, static magnetic field, Doppler effect

1. Introduction

As we well known that, in a dispersive medium, monochromatic waves propagate with different phase (v_p) velocities, while the wave package propagates with a group velocity v_g . That is, the phase velocity is related to the wave vector, \vec{k} , while the group velocity is the energy transfer velocity (carrying optical information) which is connected to the Poynting vector, \vec{S} . Mathematically, the phase velocity is determined by the relation $v_p = c/n(\omega)$, where $n(\omega)$ is the phase index and ω is the light's frequency. Meanwhile, the group velocity is defined by $v_g = c/n_g$, where n_g is the group index which

depends on the dispersion of the materials by the relation $n_g = n(\omega) + \omega[dn(\omega)/d\omega]$. In general, in the normal dispersion region with positive dispersion ($dn/d\omega > 0$), light pulses propagating with velocity $v_g \ll c$ as being 'slow light'. In contrast, in the anomalous dispersion region with negative dispersion ($dn/d\omega < 0$) so that $v_g > c$ or $v_g < 0$ which is called 'fast light' or sometimes referred to as 'backward light'. Each mode of slow light or fast light has practical applications in a number of fields such as optical telecommunication systems, optical buffers, quantum memories, magnetometers, spectrometers, radars and optical switches, etc [1].

Usually, in a certain frequency region, it is very difficult to change the dispersion properties of the medium and therefore it is difficult to change the propagation characteristics of a light pulse. However, the magnitude and the sign of the light

* Author to whom any correspondence should be addressed.

group velocity can also be easily changed by using atomic coherence and interference effects such as stimulated Brillouin scattering [2], coherent population oscillation [3] and electromagnetically induced transparency (EIT) [4]. Among these atom-coherence effects, EIT is the most interesting method and it is easily achieved experimentally [5]. It is generated from quantum interference in an atomic system when simultaneously excited by coherent laser fields. If EIT is a consequence of destructive interference, then the enhanced interference leads to an opposite effect that is EIA (electromagnetically induced absorption) [6]. As a consequence, the spectral region of EIT corresponds to the normal dispersion that allows slow light propagation, while the EIA produces anomalous dispersion that exhibits fast light propagation. On this basis, extremely slow or superluminal light pulses were obtained in the EIT [7–9] or EIA [10–12] regime, respectively. In particular, some recent studies have shown that it is possible to switch between EIT and EIA modes [13] and thus can switch between fast light and slow light by external fields such as using microwave field [14], standing-wave field [15], Kerr field [16–18], coherent pump field [19, 20], incoherent pump field [21–23], static magnetic field [24, 25], or using other coherence effects such as spontaneously generated coherence [22, 23, 26–29] and the phase of applied laser fields [30, 31] and so on.

Up to now, a lot of theoretical and experimental studies on EIT-based group velocity manipulation have been published [3, 4, 7–36]. However, most of these works are applied to ultracold atomic media with the Doppler effect being ignored. A small number of other studies were performed at room temperature with the Doppler effect included [19, 20, 31–36], which is needed for experimental and applied studies in practice.

In this work, we study the transition between fast light and slow light by the external magnetic field in a degenerate four-level atomic system for two left and right circular polarization components of the probe field. Our analytical model includes the Doppler effect and is therefore suitable for studying the group velocity of light at room temperature. The influence of laser fields and the Doppler effect on the group velocity of both polarization components of the probe field is also investigated.

2. Analytical model

We examine a four-level atomic system that is degenerated in an external magnetic field and driven by two polarized probe and coupling fields, as shown in figure 1. The two lower states $|1\rangle$ and $|2\rangle$ are the degenerate Zeeman sublevels corresponding to the magnetic quantum numbers $m_F = +1$ and $m_F = -1$ of a ground-state hyperfine level. The two upper states $|3\rangle$ and $|4\rangle$ are all the $m_F = 0$ Zeeman sublevels of different excited states, respectively. The left-circularly polarized component of the probe field E_p^- (carrier frequency ω_p and Rabi-frequency $\Omega_p^- = d_{31}E_p^-/2\hbar$ with d_{31} is electric dipole moment of the transition $|1\rangle \leftrightarrow |3\rangle$) ($m_F = +1 \leftrightarrow |3\rangle$ ($m_F = 0$)), while the right-circularly polarized component E_p^+ (with carrier frequency ω_p and Rabi-frequency

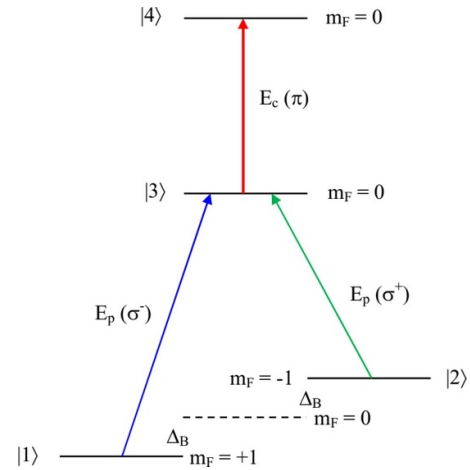


Figure 1. The degenerate four-level atomic system is placed in an external magnetic field and driven by two polarized probe and coupling fields.

$\Omega_p^+ = d_{32}E_p^+/2\hbar$) applies to the transition $|2\rangle$ ($m_F = -1$) \leftrightarrow $|3\rangle$ ($m_F = 0$). The π -polarized coupling field (with carrier frequency ω_c and Rabi-frequency $\Omega_c = d_{43}E_c/2\hbar$) interacts with the transition $|3\rangle$ ($m_F = 0$) \leftrightarrow $|4\rangle$ ($m_F = 0$). The static magnetic field (\mathbf{B}) is oriented parallel to the propagation direction of the laser fields to separate the ground state submagnetic levels through the Zeeman effect. Therefore, the Zeeman shift (Δ_B) of the ground state submagnetic levels is determined by [31]: $\hbar\Delta_B = \mu_B m_F g_F B$ where μ_B is the Bohr magneton, g_F is the Landé factor, and $m_F = \pm 1$ is the magnetic quantum number of the submagnetic states.

The time evolution of the atomic system in the laser fields is obeyed by the Liouville equation as:

$$\dot{\rho} = -\frac{i}{\hbar} [H, \rho] + \Lambda\rho, \quad (1)$$

where, the total Hamiltonian describing the atom-field interaction in the presence of static magnetic field can be written in the interaction picture as:

$$H = [(\Delta_p + \Delta_B) - (\Delta_p - \Delta_B)]|2\rangle\langle 2| + (\Delta_p + \Delta_B)|3\rangle\langle 3| + (\Delta_p + \Delta_c + \Delta_B)|4\rangle\langle 4| + \frac{\hbar}{2} (\Omega_p^- |1\rangle\langle 3| + \Omega_p^+ |2\rangle\langle 3| + \Omega_c |3\rangle\langle 4| + h.c.), \quad (2)$$

and the term $\Lambda\rho$ represents the relaxation process which is related to decay rates γ_{mn} from the state $|m\rangle$ to the state $|n\rangle$, $\Delta_p = \omega_p - \omega_{31} + \Delta_B = \omega_p - \omega_{32} - \Delta_B$ and $\Delta_c = \omega_c - \omega_{43}$ are the frequency detunings of the coupling and probe lasers, respectively.

From equations (1) and (2) we can derive the density matrix equations in the rotating-wave and electric-dipole approximations as:

$$\begin{aligned} \dot{\rho}_{31} = & -[\gamma_{31} - i(\Delta_p - \Delta_B)]\rho_{31} - \frac{i\Omega_p^-}{2}(\rho_{33} - \rho_{11}) \\ & + \frac{i\Omega_c}{2}\rho_{41} + \frac{i\Omega_p^+}{2}\rho_{21}, \end{aligned} \quad (3)$$

$$\begin{aligned} \dot{\rho}_{32} = & -[\gamma_{32} - i(\Delta_p + \Delta_B)]\rho_{32} - \frac{i\Omega_p^+}{2}(\rho_{33} - \rho_{22}) \\ & + \frac{i\Omega_c}{2}\rho_{42} + \frac{i\Omega_p^-}{2}\rho_{12} \end{aligned} \quad (4)$$

$$\dot{\rho}_{41} = -[\gamma_{41} - i(\Delta_p + \Delta_c - \Delta_B)]\rho_{41} + \frac{i\Omega_c}{2}\rho_{31} - \frac{i\Omega_p^-}{2}\rho_{43}, \quad (5)$$

$$\dot{\rho}_{42} = -[\gamma_{42} - i(\Delta_p + \Delta_c + \Delta_B)]\rho_{42} + \frac{i\Omega_c}{2}\rho_{32} - \frac{i\Omega_p^+}{2}\rho_{43} \quad (6)$$

$$\dot{\rho}_{21} = -(\gamma_{21} + i\Delta_B)\rho_{41} - \frac{i\Omega_p^-}{2}\rho_{23} + \frac{i\Omega_p^+}{2}\rho_{31}, \quad (7)$$

$$\dot{\rho}_{43} = -(\gamma_{43} - i\Delta_c)\rho_{43} - \frac{i\Omega_c}{2}(\rho_{44} - \rho_{33}) - \frac{i\Omega_p^-}{2}\rho_{41} - \frac{i\Omega_p^+}{2}\rho_{42}. \quad (8)$$

By solving the system of density matrix equations (3)–(8) in steady-state and under weak probe field approximation, the solution of density matrix elements ρ_{31} and ρ_{32} corresponding to the response of the left- and right-circularly polarized components of the probe field is found as:

$$\rho_{31} = \frac{\frac{i}{2}\Omega_p^-}{\gamma_{31} - i(\Delta_p - \Delta_B) + \frac{\frac{1}{4}\Omega_c^2}{\gamma_{41} - i(\Delta_p + \Delta_c - \Delta_B)}}, \quad (9)$$

$$\rho_{32} = \frac{\frac{i}{2}\Omega_p^+}{\gamma_{32} - i(\Delta_p + \Delta_B) + \frac{\frac{1}{4}\Omega_c^2}{\gamma_{42} - i(\Delta_p + \Delta_c + \Delta_B)}}. \quad (10)$$

From there, the expressions for the susceptibility of the atomic medium corresponding to two polarization components of the probe light can be written as:

$$\begin{aligned} \chi_p^- &= \frac{Nd_{31}^2}{2\hbar\epsilon_0\Omega_p^-}\rho_{31} \\ &\equiv \frac{iNd_{31}^2}{4\hbar\epsilon_0} \frac{1}{\gamma_{31} - i(\Delta_p - \Delta_B) + \frac{\frac{1}{4}\Omega_c^2}{\gamma_{41} - i(\Delta_p + \Delta_c - \Delta_B)}}, \end{aligned} \quad (11)$$

$$\begin{aligned} \chi_p^+ &= \frac{Nd_{32}^2}{2\hbar\epsilon_0\Omega_p^+}\rho_{32} \\ &\equiv \frac{iNd_{32}^2}{4\hbar\epsilon_0} \frac{1}{\gamma_{32} - i(\Delta_p + \Delta_B) + \frac{\frac{1}{4}\Omega_c^2}{\gamma_{42} - i(\Delta_p + \Delta_c + \Delta_B)}}. \end{aligned} \quad (12)$$

where N is the atomic density in the medium and ϵ_0 is permittivity in free space.

At the temperature T of the atomic gaseous medium, the number of atoms with velocity v is obeyed the Maxwell-Boltzmann distribution as follows:

$$N(v) = \frac{N_0}{u\sqrt{\pi}} e^{-\frac{v^2}{u^2}} dv, \quad (13)$$

where, $u = \sqrt{\frac{2k_B T}{m}}$ is the square root velocity, m is mass of the atom and N_0 is the total atomic number density in the medium.

Thus, in the presence of Doppler effect, the probe susceptibilities are modified to

$$\chi_p^-(v) dv = \frac{iN_0 d_{31}^2}{u\sqrt{\pi}\epsilon_0\hbar} \left(\frac{1}{\gamma_{31} - i(\Delta_p - \Delta_B + \frac{v}{c}\omega_p) + \frac{\frac{1}{4}\Omega_c^2}{\gamma_{41} - i(\Delta_p + \Delta_c - \Delta_B)}} \right) e^{-v^2/u^2} dv \quad (14)$$

$$\chi_p^+(v) dv = \frac{iN_0 d_{32}^2}{u\sqrt{\pi}\epsilon_0\hbar} \left(\frac{1}{\gamma_{32} - i(\Delta_p + \Delta_B + \frac{v}{c}\omega_p) + \frac{\frac{1}{4}\Omega_c^2}{\gamma_{42} - i(\Delta_p + \Delta_c + \Delta_B)}} \right) e^{-v^2/u^2} dv. \quad (15)$$

By integrating the expressions (14) and (15) over the velocity v from $-\infty$ to $+\infty$ yields the following results:

$$\chi_p^- = \frac{iNd_{31}^2\sqrt{\pi}}{\epsilon_0\hbar\left(\frac{\omega_p u}{c}\right)} \left[e^{z_1^2} (1 - \text{erf}(z_1)) \right], \quad (16)$$

$$\chi_p^+ = \frac{iNd_{32}^2\sqrt{\pi}}{\epsilon_0\hbar\left(\frac{\omega_p u}{c}\right)} \left[e^{z_2^2} (1 - \text{erf}(z_2)) \right], \quad (17)$$

where,

$$z_1 = \frac{c}{\omega_p u} \left(\gamma_{31} + i(\Delta_p - \Delta_B) + \frac{\frac{1}{4}\Omega_c^2}{\gamma_{41} + i(\Delta_p + \Delta_c - \Delta_B)} \right), \quad (18)$$

$$z_2 = \frac{c}{\omega_p u} \left(\gamma_{32} + i(\Delta_p + \Delta_B) + \frac{\frac{1}{4}\Omega_c^2}{\gamma_{42} + i(\Delta_p + \Delta_c + \Delta_B)} \right), \quad (19)$$

and, $\text{erf}(z)$ is the error function with complex argument z which is defined by:

$$\text{erf}(z) = \frac{2}{\sqrt{\pi}} \int_0^z e^{-t^2} dt. \quad (20)$$

According to the Kramers-Kronig relation, the dispersion and absorption coefficients of the two circularly polarized

probe components are directly proportional to the real $\text{Re}(\chi_p)$ and imaginary $\text{Im}(\chi_p)$ parts of the susceptibility, as follows:

$$\alpha = \frac{\omega_p \text{Im}(\chi_p)}{c}, \quad (21)$$

$$n = 1 + \frac{\text{Re}(\chi_p)}{2}. \quad (22)$$

The group index of the medium for the probe light can be determined as:

$$n_g = n + \omega_p \frac{\partial n}{\partial \omega_p}. \quad (23)$$

And the group velocity v_g of the probe light is related to n_g as follows:

$$v_g = \frac{c}{n_g}. \quad (24)$$

3. Results and discussion

As a theoretical model recommendation for experimental realization with the ^{87}Rb atom, the excitation diagram with the relevant energy levels of ^{87}Rb atom is shown in figure 2. In which, the left-circularly polarized probe field (σ^-) excites the atom on the transition $|5S_{1/2}, F=1, m_F=1\rangle \rightarrow |5P_{1/2}, F=1, m_F=0\rangle$ and the right-circularly polarized probe field (σ^+) interacts with the transition $|5S_{1/2}, F=1, m_F=-1\rangle \rightarrow |5P_{1/2}, F=1, m_F=0\rangle$, while the π -polarized coupling field applies to the transition $|5P_{1/2}, F=1, m_F=0\rangle \rightarrow |5D_{3/2}, F=2, m_F=0\rangle$. For convenience in simulation, all physical quantities with frequency units are normalized by γ that are of the order of MHz for rubidium sodium atoms. In this way, when the Zeeman shift Δ_B is scaled by γ , then the magnetic field strength B should be in units of the combined constant $\gamma_c = \gamma \hbar / (\mu_B g_F)$ that also has the units of the Tesla. For example, when the magnetic field strength $B = 3\gamma_c$, the Zeeman shift received is $\Delta_B = 3\gamma$. In addition, we also note that the external magnetic field has no effect on the $m_F = 0$ states, so the transition of the π -polarized light is also not affected by the magnetic field. The atomic parameters can be chosen as [34]: $N = 7 \times 10^{17}$ atoms m^{-3} , $\gamma_{31} = \gamma_{32} = 5.3$ MHz, $d_{31} = 1.6 \times 10^{-29}$ C·m. We also note that the boiling point of rubidium is about 39°C [37], so that at room temperature it exists in a gaseous state and is therefore influenced by Doppler broadening significantly.

Using expressions (16) and (17) we simulate the left- and right-circularly polarized probe absorption spectra at room temperature in the absence of a magnetic field as shown in figure 3. It is obvious at room temperature the linewidth of EIT due to Doppler effect is relatively large and has the order of GHz (about 100 times larger than the case of free-Doppler), so it is difficult to observe the EIT window. At the same time, to achieve the phenomenon of EIT, it is required that the coupling field intensity is also large enough (for example, in this case $\Omega_c = 40\gamma$). In addition, in the absence of the magnetic

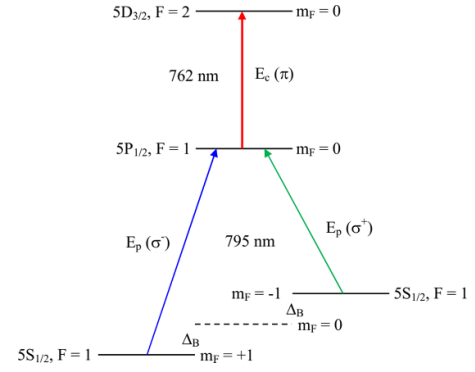


Figure 2. Related energy levels of ^{87}Rb atom in the external magnetic field and the excitations of the laser fields on the atomic transitions.

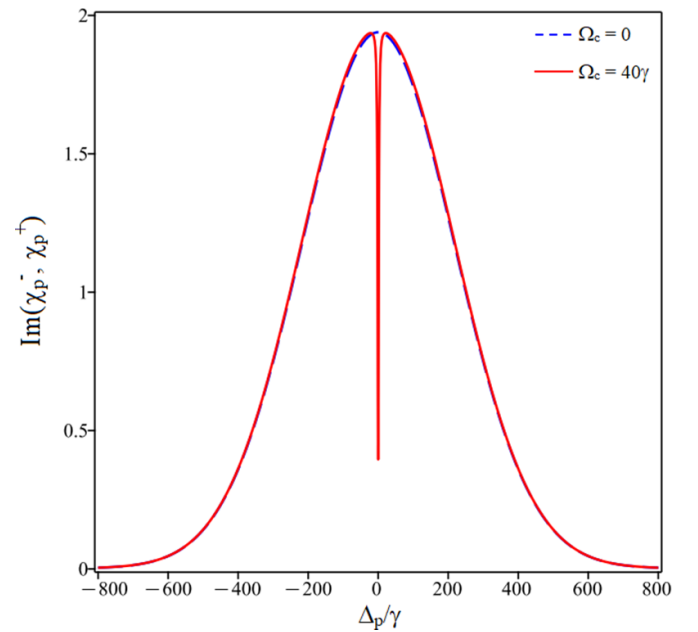


Figure 3. Left- and right-circularly polarized probe absorption spectra at room temperature $T = 300$ K in the absence of the magnetic field $B = 0$. The coupling field parameters as $\Omega_c = 0$ (dashed line) and $\Omega_c = 40\gamma$ (solid line) and $\Delta_c = 0$.

field, the left- and right-circularly polarized probe absorption spectra is overlapped and two EIT window are located at the resonant frequency $\Delta_p = 0$.

In figure 4, we investigate the influence of the magnetic field on the EIT spectra of left- and right- circularly polarized probe field at room temperature. In this case, we selected the external field strength $B = 3\gamma_c$, so that the EIT window of the left-circularly polarized probe field is shifted to the right side by an amount of 3γ and is located at the position $\Delta_p = 3\gamma$, while the EIT window of the right- circularly polarized probe field is shifted to the left side by 3γ and is located at the position $\Delta_p = -3\gamma$. This shift of the EIT positions changes the optical response of the medium, specifically at the resonant probe frequency the transparency is converted to the absorption, while at the probe frequency corresponding to $\Delta_p = +3\gamma$

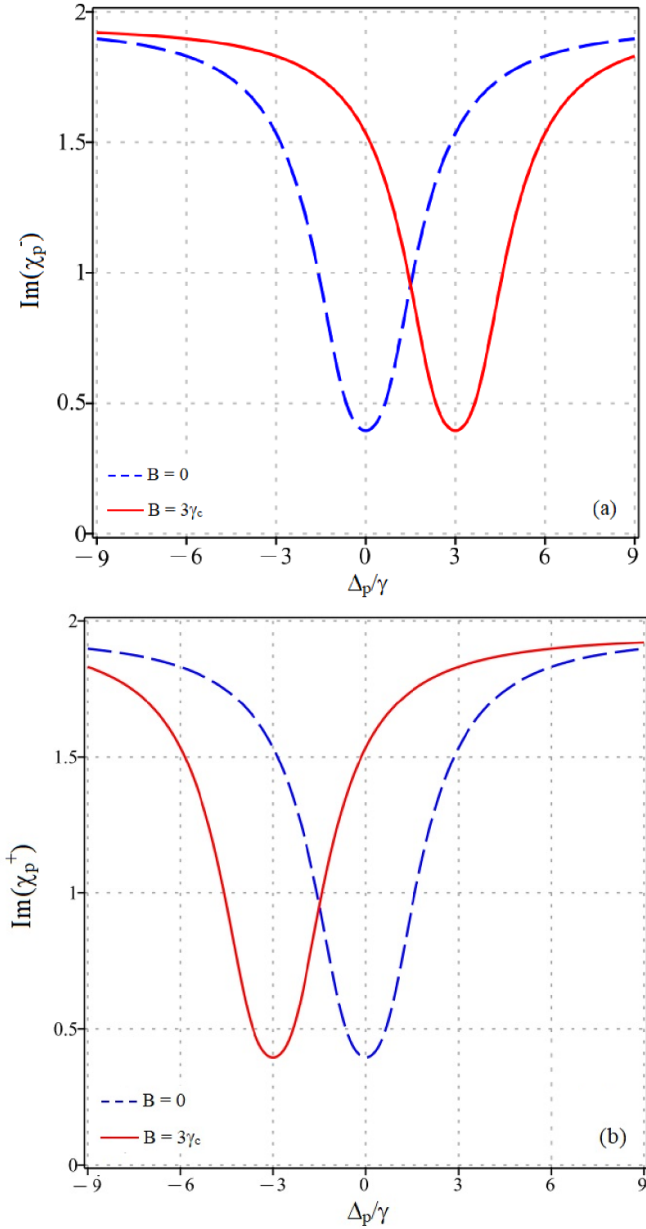


Figure 4. (a) Left- and (b) right- circularly polarized probe absorption spectra at room temperature $T = 300$ K in the absence and presence of the magnetic field: $B = 0$ (dashed line) and $B = 3\gamma_c$ (solid line). The coupling field parameters as $\Omega_c = 40\gamma$ and $\Delta_c = 0$.

(left-circularly polarized component) or $\Delta_p = -3\gamma$ (right-circularly polarized component) the absorption is switched to the transparency. This is the basis for the transition between slow light and fast light by the external magnetic field, which will be investigated in figures 4 and 5 below.

Figure 5 is made similar to figure 4 but the investigation is for the group index. As we know that, in the EIT region the medium exhibits normal dispersion, so the group index has a positive value (corresponding to slow light), whereas in the absorption region the medium exhibits anomalous dispersion and hence the group index has a negative value (fast light). For example, at the resonant probe frequency corresponding to $\Delta_p = 0$, the group index reaches a positive extreme in the

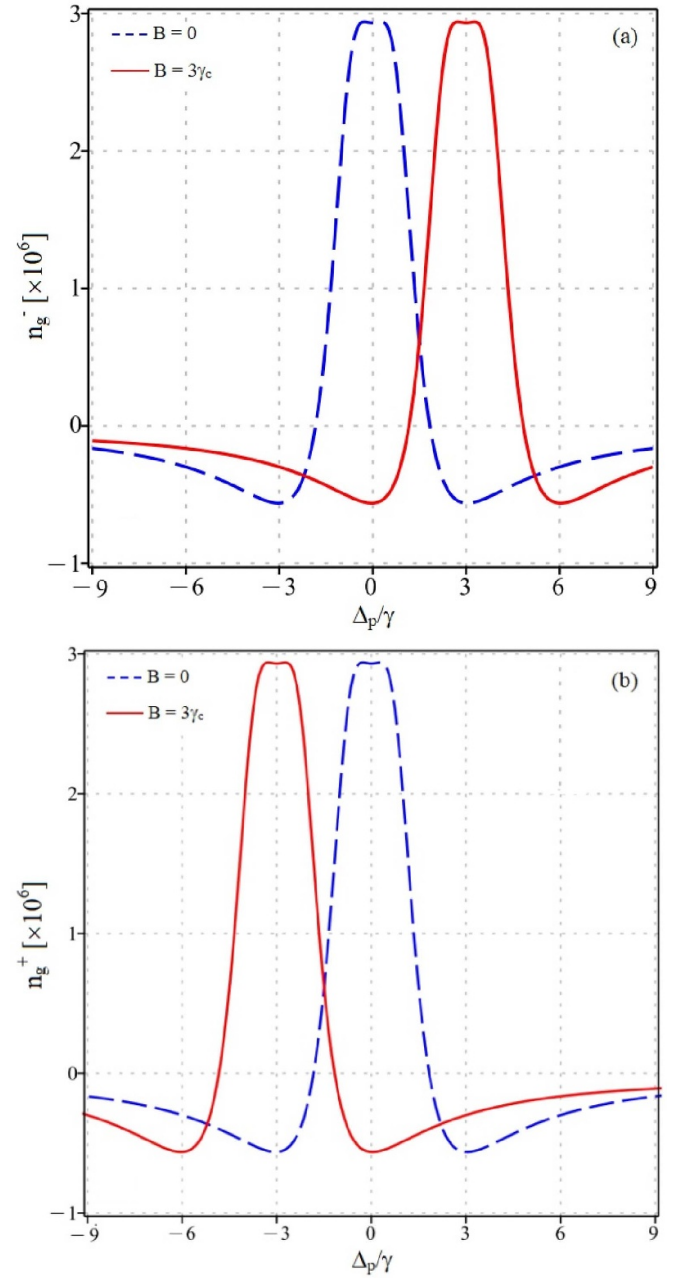


Figure 5. (a) Variations of group index n_g versus the frequency detuning Δ_p for (a) left- and (b) right- circularly polarized probe field at room temperature $T = 300$ K in the absence and presence of the magnetic field $B = 0$ (dashed line) and $B = 3\gamma_c$ (solid line). The coupling field parameters as $\Omega_c = 40\gamma$ and $\Delta_c = 0$.

absence of magnetic field and a negative extreme in the presence of magnetic field, whereas at the probe frequency corresponding to $\Delta_p = +3\gamma$ (left-circularly polarized component) or $\Delta_p = -3\gamma$ (right-circularly polarized component) the group index reaches the negative extreme in the absence of magnetic field and the positive extreme in the presence of magnetic field. Thus, we can change the value of the group index from the positive extreme to the negative one and vice versa by the external magnetic field. More specifically, we fixed the probe frequency at the atomic resonance frequency ($\Delta_p = 0$)

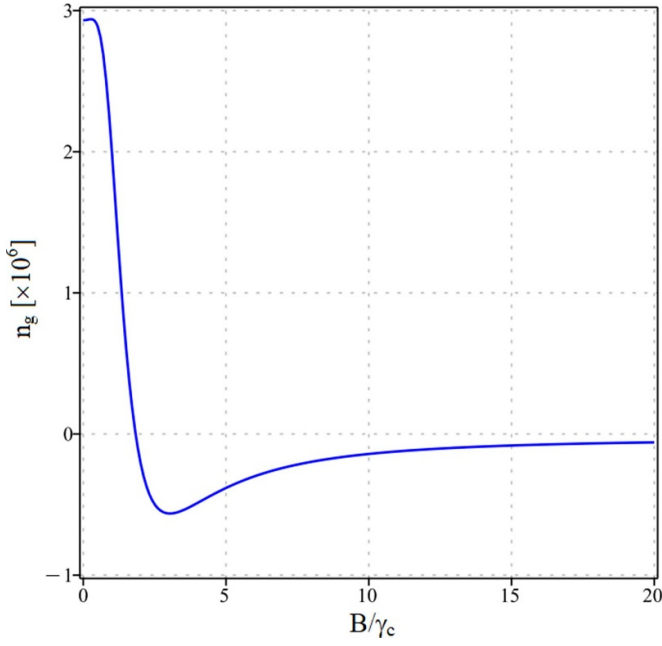


Figure 6. (a) Variation of group index n_g versus the magnetic field B at room temperature $T = 300$ K. Other parameters as $\Omega_c = 40\gamma$, $\Delta_c = 0$ and $\Delta_p = 0$.

and plotted the group index with respect to the magnetic field B as shown in figure 6. It also sees that the value of the group index varies continuously from the positive extreme to the negative extreme as the magnetic field increases. This means that we can use the static magnetic field to switch the mode of light propagation between fast and slow or vice versa.

Besides, the group index has controlled according to the external magnetic field, it is also variable with respect to the coupling field strength as shown in figure 7 for the right-circularly polarized probe field with the magnetic field $B = 3\gamma_c$. As investigated in figure 7(a), at resonant probe frequency $\Delta_p = 0$ the group index varies from zero to the negative extreme then to positive extreme when the coupling Rabi frequency (coupling field intensity) varies from zero to about 80γ (passing the value $\Omega_c = 55\gamma$, the group index changes its sign), then it gradually decreases as the coupling Rabi frequency continues to increase. Thus, the group index changes both magnitude and sign when changing the coupling field intensity. Figure 7(b) shows the group index as a function of the probe frequency detuning at different coupling Rabi frequencies in the case of magnetic field $B = 3\gamma_c$. It is shown that, at the probe frequency corresponding to the frequency detuning $\Delta_p = 3\gamma$, the peak of the group index is reduced as the coupling field intensity increases, at the same time the profile of the group index is expanded due to the power broadening. The increase in laser coupling strength leads to the extension of the EIT window thereby reducing the slope of the dispersion curve [5, 34], which is the reason for the decrease in the amplitude of the group refractive index as we see in figure 7(b).

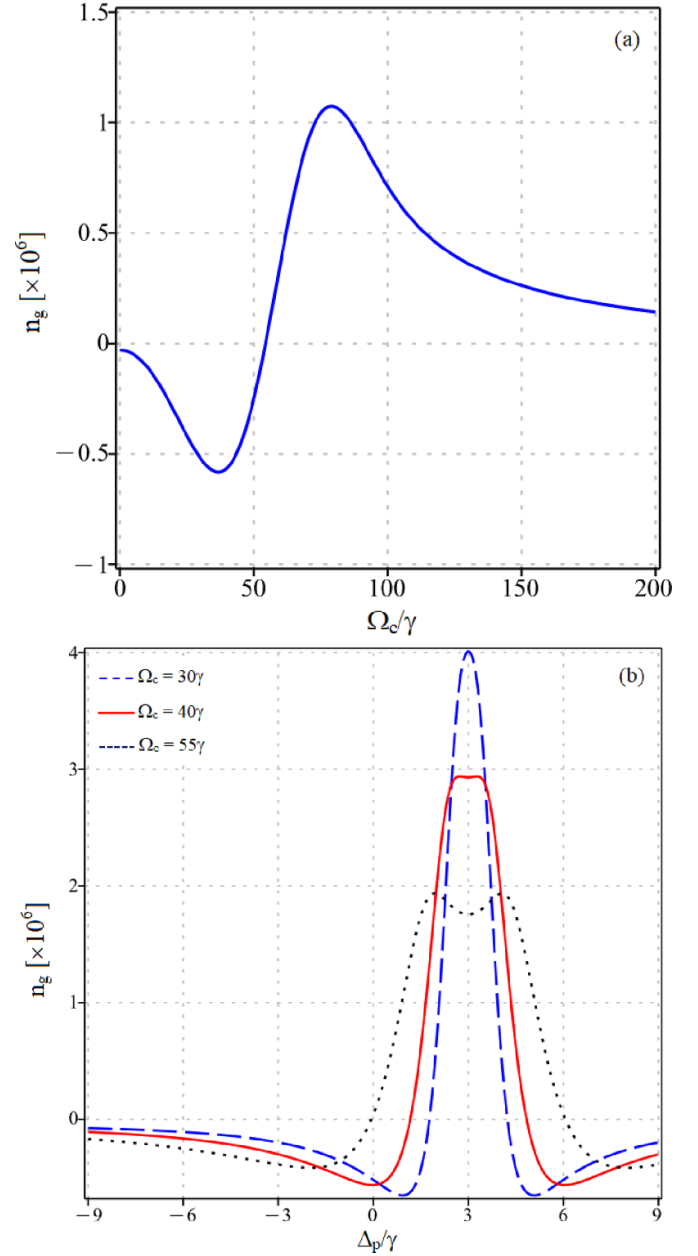


Figure 7. (a) Variation of group index n_g versus the coupling Rabi frequency Ω_c at room temperature $T = 300$ K and in the presence of magnetic field $B = 3\gamma_c$ while laser field parameters are fixed as $\Delta_p = \Delta_c = 0$. (b) Variations of group index n_g versus the frequency detuning Δ_p (for left-circularly polarized probe field) in the presence of magnetic field $B = 3\gamma_c$ at different coupling Rabi frequencies: $\Omega_c = 30\gamma$ (dashed line), $\Omega_c = 40\gamma$ (solid line) and $\Omega_c = 55\gamma$ (dotted line).

Finally, in figure 8 we investigate the influence of Doppler effect (or temperature) on the group index. In figure 8(a), we plotted the group index at resonant probe frequency $\Delta_p = 0$ versus the temperature T with the magnetic field $B = 3\gamma_c$. It is clear that the temperature of the atomic medium also has a significant effect on the group index, specifically increasing the temperature reduces the amplitude of the group index and even changes the sign of the group index or changes the probe

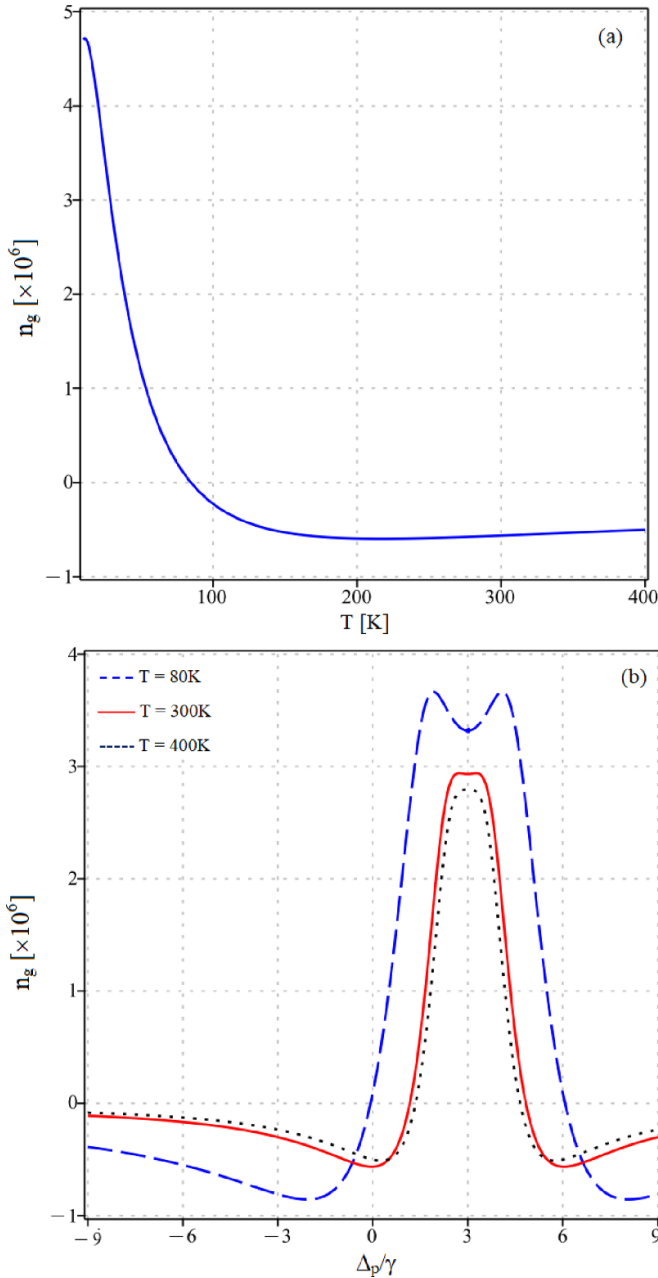


Figure 8. (a) Variation of group index n_g versus temperature T in the presence of magnetic field $B = 3\gamma_c$ at laser field parameters are fixed as $\Omega_c = 40\gamma$, $\Delta_c = 0$ and $\Delta_p = 0$. (b) Variations of group index n_g versus the frequency detuning Δ_p (for left-circularly polarized probe field) in the presence of magnetic field $B = 3\gamma_c$ at different temperatures: $T = 80$ K (dashed line), $T = 300$ K (solid line) and $T = 400$ K (dotted line), and the coupling field parameters as $\Omega_c = 40\gamma$ and $\Delta_c = 0$.

light propagation regime in the medium (for example, as the temperature passing $T = 80$ K, the group index changes its sign). The decrease in the amplitude of the group index with increasing temperature is also seen in figure 8(b) at the probe frequency corresponding to the frequency detuning $\Delta_p = 3\gamma$. The fact that the increase in temperature reduces the transparency efficiency and thus the amplitude of group index also decreases inside the EIT spectral region.

4. Conclusion

We have developed the analytical model of a degenerate four-level atomic system under an external magnetic field to study the control of EIT phenomenon and group index/group velocity at room temperature. The expressions for the susceptibility and the group index for the left- and right- circularly polarized components of the probe field were found as a function of the laser parameters, atomic parameters, magnetic field strength and atomic temperature. The external magnetic field does not change the EIT linewidth, but it does shift the position of the EIT window around the resonant frequency. At room temperature, the absorption profile of the probe field is greatly expanded due to the Doppler effect, so the EIT window as well as the EIT shift are more difficult to observe. Also, sufficiently large coupling field intensity is required to produce an EIT phenomenon compared with the free-Doppler case. In particular, by choosing the appropriate magnetic field strength, the optical response of the medium to the probe field can be changed from transparency to absorption and vice versa. Consequently, the amplitude of the group index also varies from the positive extreme to the negative extreme and vice versa, and thus the propagation of the probe light is also switched between the fast and slow light regimes. In addition, at a given magnetic field, the value of the group index is also changed in both magnitude and sign by the coupling field intensity. Furthermore, our analytical model allows easy investigation of the influence of atomic temperature on the group index. The investigation shows that the temperature of the medium has a significant effect on the group index, which changes not only the amplitude but also the sign of the group index as the temperature increases. Our calculation can be useful for experimental observation and related applications at room temperature.

Data availability statement

No new data were created or analysed in this study.

Acknowledgments

This work is supported by Vietnam’s Ministry of Education and Training under Grant No. B2022-TDV-05, and Vingroup Innovation Foundation (VINIF) under project code VINIF.2022.DA00076.

ORCID iDs

Nguyen Huy Bang  <https://orcid.org/0000-0003-4702-3157>
 Le Van Doai  <https://orcid.org/0000-0002-1850-3437>

References

- [1] Boyd R W 2009 Slow and fast light: fundamentals and applications *J. Mod. Opt.* **56** 1908

- [2] Herráez González M, Song K Y and Thévenaz L 2005 Optically-controlled slow and fast light in optical fibers using stimulated Brillouin scattering *Appl. Phys. Lett.* **87** 081113
- [3] Gonzalo I, Antón M A, Carreño F and Calderón Oscar G 2008 Subluminal and superluminal propagation in a three-level atom in the radiative limit based on coherent population oscillations *Phys. Lett. A* **372** 6334–9
- [4] Hau L V, Harris S E, Dutton Z and Behroozi C H 1999 Light speed reduction to 17 metres per second in an ultracold atomic gas *Nature* **397** 594–8
- [5] Huy B N, Le Van D and Xuan K D 2019 Controllable optical properties of multiple electromagnetically induced transparency in gaseous atomic media *Commun. Phys.* **28** 1–33
- [6] Lezama A, Barreiro S and Akulshin A M 1999 Electromagnetically induced absorption *Phys. Rev. A* **59** 4732–5
- [7] Han D, Zeng Y, Bai Y, Cao H, Chen W, Huang C and Lu H 2008 Controlling the group velocity in a five-level K-type atomic system *Opt. Commun.* **281** 4712–4
- [8] Bencheikh K, Baldit E, Briaudeau S, Monnier P, Levenson J A and Mélin G 2010 Slow light propagation in a ring erbium-doped fiber *Opt. Express* **18** 25642–8
- [9] Ali H and Ahmad I 2014 The effect of Kerr nonlinearity and Doppler broadening on slow light propagation *Laser Phys.* **24** 025201
- [10] Wang L J, Kuzmich A and Dogariu A 2000 Gain-assisted superluminal light propagation *Nature* **406** 277
- [11] Dogariu A, Kuzmich A and Wang L J 2001 Transparent anomalous dispersion and superluminal light-pulse propagation at a negative group velocity *Phys. Rev. A* **63** 053806
- [12] Akulshin A M and McLean R J 2010 Fast light in atomic media *J. Opt.* **12** 104001
- [13] Yadav K and Wasan A 2019 Switching from EIT to EIA in a four-level N-type atomic system *J. Opt.* **48** 65–69
- [14] Agarwal G S, Dey T N and Menon S 2001 Knob for changing light propagation from subluminal to superluminal *Phys. Rev. A* **64** 053809
- [15] Bae I H and Moon H S 2011 Continuous control of light group velocity from subluminal to superluminal propagation with a standing-wave coupling field in a Rb vapor cell *Phys. Rev. A* **83** 053806
- [16] Dey T N and Agarwal G S 2007 Observable effects of Kerr nonlinearity on slow light *Phys. Rev. A* **76** 015802
- [17] Anh N T, Doai L V and Bang N H 2018 Manipulating multi-frequency light in a five-level cascade type atomic medium associated with giant self-Kerr nonlinearity *J. Opt. Soc. Am. B* **35** 1233–9
- [18] Doai L V 2020 The effect of giant Kerr nonlinearity on group velocity in a six-level inverted-Y atomic system *Phys. Scr.* **95** 035104
- [19] Kuang S, Wan R, Kou J, Jiang Y and Gao J 2009 Switching from subluminal to superluminal light propagation via a coherent pump field in a four-level atomic system *J. Opt. Soc. Am. B* **26** 2256
- [20] Bharti V and Natarajan V 2017 Sub- and super-luminal light propagation using a Rydberg state *Opt. Commun.* **392** 180–4
- [21] Mahmoudi M, Sahrai M and Tajalli H 2006 The effects of the incoherent pumping field on the phase control of group velocity *J. Phys. B: At. Mol. Opt. Phys.* **39** 1825–35
- [22] Dutta S 2011 The incoherent pump rate: an optical tool for controlling the probe response and dispersion in a three-level Λ system in the presence of spontaneously generated coherence *Phys. Scr.* **83** 015401
- [23] Anh L N M, Bang N H, Phu N V, Dong H M, Hien N T T and Doai L V 2023 Slow light amplification in a three-level cascade-type system via spontaneously generated coherence and incoherent pumping *Opt. Quantum Electron.* **55** 246
- [24] Asadpour S H, Hamedani H R and Soleimani H R 2015 Slow light propagation and bistable switching in a graphene under an external magnetic field *Laser Phys. Lett.* **12** 045202
- [25] Phu N V, Bang N H and Doai L V 2021 Controlling group velocity via an external magnetic field in a degenerated three-level lambda-type atomic system *Photonics Lett. Pol.* **13** 13–15
- [26] Carreño F, Calderón Oscar G, Antón M A and Gonzalo I 2005 Superluminal and slow light in Λ -type three-level atoms via squeezed vacuum and spontaneously generated coherence *Phys. Rev. A* **71** 063805
- [27] Han D, Zeng Y, Chen W, Cao H and Lu H 2009 Sub- and superluminescence with gain in a three-level ladder-type atomic system with spontaneously generated coherence *J. Mod. Opt.* **56** 2357–62
- [28] Bang N H, Anh L N M, Dung N T and Doai L V 2019 Comparative study of light manipulation in three-level systems via spontaneously generated coherence and relative phase of laser fields *Commun. Theor. Phys.* **71** 947–54
- [29] Anh L N M, Bang N H, Phu N V, Khoa D X, Ngan N T, Huyen B T and Doai L V 2023 Influence of spontaneously generated coherence on absorption, dispersion, and group index in a five-level cascade atomic system *Phys. Scr.* **98** 045106
- [30] Yang W-X, Ma W-H, Yang L, Zhang G-R and Lee R-K 2014 Phase control of group velocity via Fano-type interference in a triple semiconductor quantum well *Opt. Commun.* **324** 221–6
- [31] Qiu T-H and Xie M 2016 Phase control of group velocity in a Doppler-broadened -type three-level system *Int. J. Theor. Phys.* **55** 2942–8
- [32] Bharti V and Wasan A 2014 Complete wavelength mismatching effect in a Doppler broadened Y-type six-level EIT atomic medium *Opt. Commun.* **324** 238–44
- [33] Yadav K and Wasan A 2017 Sub-luminal and super-luminal light propagation in inverted-Y system with wavelength mismatching effects *Phys. Lett. A* **381** 3246–53
- [34] Anh N T, Doai L V, Son D H and Bang N H 2018 Manipulating multi-frequency light in a five-level cascade EIT medium under Doppler broadening *Optik* **171** 721–7
- [35] Bigelow M S, Lepeshkin N N and Boyd R W 2003 Superluminal and slow light propagation in a room-temperature solid *Science* **301** 200
- [36] Mirza Azeem B and Singh S 2016 Subluminal and superluminal light propagation via electromagnetically induced transparency in radiatively and inhomogeneously broadened media *J. Mod. Opt.* **64** 716–24
- [37] Steck D A 2019 ⁸⁷Rb D Line Data (available at: <http://steck.us/alkalidata>)